SNRU Journal of Science and Technology

Journal home page: snrujst.snru.ac.th

Fabrication of PVDF/PVP nanofiltration membrane containing chitosan/activated carbon/Ag nanoparticles by electrospinning and their antibacterial activity

Ronariddh Nakhowong[1, 2], Sirinun Wiriyasoontorn[3], Amornrat Wongklom[3], Aroon Jankam[3], Nualyai Yaraksa[3], Romteera Chueachot[2, 3,*]

[1]Program of Physics, Faculty of Science, Ubon Ratchathani Rajabhat University, Ubon Ratchathani 34000 Thailand

[2]Functional Nanomaterials and Electrospinning Research Laboratory, Faculty of Science, Ubon Ratchathani Rajabhat University, Ubon Ratchathani 34000 Thailand

[3]Program of Chemistry, Faculty of Science, Ubon Ratchathani Rajabhat University, Ubon Ratchathani 34000 Thailand

[*]**Corresponding Author**: romteera.c@ubru.ac.th

Received: 3 September 2019; **Revised:** 13 November 2019; **Accepted:** 15 November 2019; **Available online:** 1 January 2019

Abstract

Polyvinylidene fluoride (PVDF)/poly(vinylpyrrolidone)(PVP) nanofiltration membranes containing chitosan/activated carbon/silver nanoparticles were fabricated by electrospinning. Different amount of silver nanoparticles (AgNPs) (x = 0, 0.20, 0.30, 0.40 and 0.5 %v v^{-1}) were added to PVDF/PVP/chitosan(CS)/activated carbon (AC) solution. The composite fibrous membranes were characterized by field emission scanning electron microscopy (FESEM), UV-Vis spectroscopy (UV-Vis), and attenuated total reflection Fourier transform infrared spectroscopy (ATR-FTIR). FESEM images showed that the fibrous membranes had rough surfaces with random distribution and average fiber diameter ranging from 0.90 to 1.80 µm. For the composite fibrous membranes, average diameter increases as the amount of Ag nanoparticles increased. UV-Vis spectrum exhibited surface plasmon resonance band at 389 nm. Zetasizer measurement showed average diameter of AgNPs as 30 nm. Performances of the composite membrane were assessed by vacuum filtration. Silica (SiO_2) particles with diameters of 0.10 – 0.60 µm were used to test the filtration efficiency. After filtration, silica particles with sizes ranging from 0.20 – 0.35 µm were detected, indicating that composite membranes effectively filtrated silica particles and bacteria with size over 0.35 µm. ATR-FTIR showed dominant absorption peaks corresponding to PVDF and PVP. Antibacterial activities of the composite membrane were tested against *Staphylococcus aureus* and *Escherichia coli* following the filtration method. Results confirmed excellent antibacterial performance of composite membranes containing AgNPs against *Escherichia coli*, with potential promising candidates for purifying drinking purified water and other applications.

Keywords: PVDF/PVP membrane; Silver nanoparticles; Chitosan; Antibacterial; Electrospinning

1. Introduction

Membrane separation technology has recently received considerable research attention. Membrane separation offers environmentally friendly, low energy consumption, high separation efficiency technology that can be applied in drinking water and wastewater treatment including food, chemical, medicine, and biotechnology [1]. Improvement of fresh water resources using more efficient and low cost water treatment methods is urgently required to address the critical issue of ever growing water demands [2]. A membrane acts as a barrier between two phases that allows substances to be

selectively transported from one side to the other [2]. Membranes are classified as porous or dense, depending on their structure [3]. There are many significant advantages of using membranes for industrial processes such as no phase changes or chemical additives, modular which is easy to scale up, simple in operation, relatively low energy consumption, etc. [3]. Water treatment methods and processes have recently attracted increasing attention due to the necessity of fresh clean water for everyday life. Membranes can be classified depending on their pore size as microfiltration (MF), ultrafiltration (UF), nanofiltration (NF) and reverse osmosis/forward osmosis separation methods [1, 3]. MF membranes separate or reject particles from about 0.05 – 0.10 μm to 1.00 μm and are effective for the removal of protozoa and bacteria, while UF membranes remove particles in the range of 0.01 – 0.10 μm and are usually used to remove viruses, emulsified oils, metal hydroxides, colloids, proteins, and other large molecular weight materials from water and other solutions. NF membranes remove particles in the range of 0.50 – 2.00 nm, their advantages include high-solute rejection and low-energy consumption [1]. Electrospinning is a new, simple, versatile and cost-effective method for fabricating fibrous materials with diameters ranging from several micrometers to nanometers. Recently, fibrous membranes have received considerable attention in the field of water purification and water distillation due to their intrinsic properties such as high surface areas, mechanical stability and controllable fiber size which allow entry of composite materials into the nanofibrous matrix. Silver nanoparticles are now used in various applications such as biomedical, electrical, catalysis, energy, environmental and filtration [4]. AgNPs have unique characteristics which include effectiveness against a vast range of antibiotic resistant bacteria, efficient and easy incorporation into polymer matrices, and low human toxicity compared to other heavy metals [5]. AgNPs are preferred for dispersion in nanofibers as they offer high-performance applications such as long-term antibacterial effect, long lifetime and high enhancement sensitivity of Raman scattering [6]. Chitosan exhibits a wide spectrum of antibacterial activities against both gram-positive and gram-negative bacteria [7]. Activated acarbon is widely used as adsorbents, catalysts and catalyst supports for the removal of pollutant species from gases or liquids and for purification or recovery of the chemicals [8]. Membrane porosity of the composite membrane (ε) was determined by the gravimetric method and calculated by equations (1);

$$\varepsilon = \frac{m_1 - m_2}{\rho \cdot A \cdot l} \tag{1}$$

where m_1 and m_2 are the weight of the wet composite membrane and dry composite membrane, respectively, A and l are the area of membrane sample and the thicknesses of the composite membrane (measured with a micrometer), respectively, and ρ is the density of PVDF/PVP [9].

PVDF/PVP nanofiltration membranes containing chitosan/activated carbon/AgNPs were fabricated by electrospinning. Different amount of added AgNPs were investigated for filtration efficiency. Antibacterial activity of the composite membrane was tested using Gram-negative bacteria of *Escherichia coli* and Gram-positive bacteria of *Staphylococcus aureus* by the filtration method.

2. Materials and methods

Materials

Polyvinylidene fluoride (PVDF, Mw = 530,000 g mol^{-1}), and poly(vinylpyrrolidone) (PVP, Mw = 1,300,000 g mol^{-1}) were purchased from Sigma Aldrich. Silver nitrate ($AgNO_3$), acetone, acetic acid and *N,N*-dimethylformaminde (DMF) were purchased from Carlo Erba. Sodium borohydride ($NaBH_4$) was purchased from Acros, while chitosan (DAC, Mw = 15,000 g mol^{-1}, 90%) was purchased from Seafresh Chitosan (Lab) Company Ltd. Activated carbon (CA) was purchased from Giant Leo Intertrade Co., Ltd. All chemical reagents were analytical grade and used as received with no further purification.

Preparation the chitosan solution and AgNPs

A 1 % chitosan (CS) solution was prepared in distilled water. First, 1 mL of acetic acid was added in 98 mL of distilled water with magnetic stirring. Then, 1 g of chitosan powders was added and magnetic stirring was continued at room temperature for 24 h to obtain a clear solution. To synthesize AgNPs, 0.001 M $AgNO_3$ solution and 0.002 M $NaBH_4$ were prepared in distilled water. Then, 30 mL of $NaBH_4$ was placed an ice bath at below 5 °C and 10 mL of $AgNO_3$ solution was slowly added dropwise with vigorous stirring to achieve the AgNPs. After cooling to room temperature, the solution was shielded from light to preserve the AgNPs and small amount of PVP solution was added to prevent agglomeration of the AgNPs.

Preparation of composite nanofiltration membrane

A sample of 16 wt.% of PVDF solution was prepared in DMF and acetone (acetone : DMF = 3 : 1 v v^{-1}) with magnetic stirring at 50 °C for 6 h. Then, 12 wt.% PVP solution was prepared in DMF and acetone (acetone : DMF = 3 : 1 v v^{-1}) with magnetic stirring at room temperature for 2 h. Finally, a PVDF/PVP (3 : 1) solution was blended with stirring at 50 °C for 12 h to obtain a clear liquid. Different amount of AgNPs contents at 0 (PVDF/PVP), 0.20 (Ag200), 0.30 (Ag300), 0.40 (Ag400) and 0.5 %v v^{-1} (Ag500) were added into the PVDF/PVP solution and stirred for 12 h to ensure a complete dispersion of the mixture solution. Next, 0.20 %v v^{-1} of CS and 50 mg AC were added in above solution. The solution mixture was loaded into a 10 mL plastic syringe with a needle (ID = 0.60 mm) and mounted on a syringe pump in the electrospinning system. The needle tip was connected to the positive electrode terminal of a high voltage power supply (Gamma High Voltage Research, ES30P-5W). The negative electrode terminal was connected to the rotating collector which was covered with aluminum foil. A high voltage of 16 kV was applied to the needle tip with the collector separated at 15 cm. Feed rate of the solution was set at 1.50 mL min^{-1}.

Characterization

Surface morphology of the fibrous membrane was observed by a field emission scanning electron microscopy (FESEM, JSM-7610FPlus, JOEL). Chemical structure and functional groups of the samples were determined by attenuated total reflection Fourier transform infrared spectroscopy (ATR-FTIR, Tensor II, Bruker) in wavenumber range from 4,000 – 400 cm^{-1}. Optical properties of the AgNPs were analyzed by a UV–Vis spectrophotometer (T90+, PG Instruments). Particle sizes of the samples were measured by a Zetasizer (Malvern, Nano-ZS90).

Antibacterial test

Antibacterial properties of the composites membranes were tested by the filtration technique using Gram-positive *Staphylococcus aureus* (*S. aureus*, ATCC25923) and Gram-negative *Escherichia coli* (*E. coli*, ATCC25922) bacteria. The fibrous membranes were autoclaved at 120 °C for 20 min and kept in a biosafety cabinet at room temperature. *E.coli* and *S. aureus* were prepared at optimal density (OD) 0.10 and wavelength 625 nm before dilution with distilled water at 10^{-5} CFU mL^{-1} and filtration by the composite membranes at different AgNP contents. Then, *E. coli* and *S. aureus* were subcultured on plate count agar by pour plate technique and incubated at 37 °C for 24 h. Quantitative and qualitative antibacterial assays were performed by counting colony forming units per mL (CFU/mL^{-1}) and imaged with a digital camera. Finally, surviving colonies were observed after the filtration test. The PVDF/PVP membrane was used as a control.

3. Results and discussion

Photographic images of the composite membrane at different AgNPs contents are shown in Fig. 1. The PVDF/PVP membrane (Fig. 1(a)) had a bright color due to the nature of polymer. After the composite materials were added, the composite membrane has turned darker due to incorporation of

AC (black); however, intensity of the dark color decreased as the quantity of AgNPs increase (Fig. 1(b – e)).

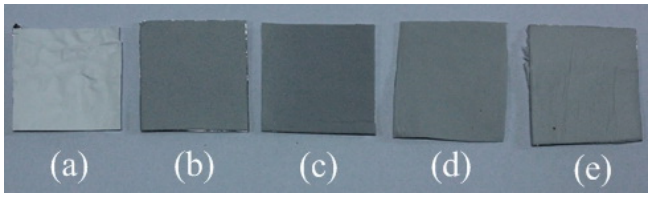

Fig. 1 Photograph images of fibrous membrane: (a) PVDF/PVP, (b) PVDF/PVP/CS/AC membrane contains AgNPs at 0.2, (c) 0.3, (d) 0.4, and (e) 0.5 %v v^{-1}.

FESEM was used to evaluate the surface morphology of the obtained membrane as shown in Fig. 2. The FESEM image of the PVDF/PVP membrane (Fig. 2(a)) exhibited a relatively smooth surface with no beads or breakage and average diameter of 0.92 ± 0.18 µm. After CS, AC, and different AgNP contents were added into the PVDF/PVP membrane, fiber diameter increased as AgNP contents increased, indicating that concentration of AgNPs exhibited a significant role in controlling the fiber diameter (Fig. 2(b – e)). FESEM images exhibited a fully interconnected pore structure with several pore size distributions. Average diameters of Ag200, Ag300, Ag400, and Ag500 were 1.44 ± 0.35, 1.53 ± 0.52, 1.55 ± 0.37, and 1.77 ± 0.64 µm, respectively, which correspond to Kang et. [10]. The surface morphology exhibited remarkable roughness, which increased with increasing amounts of AgNP contents. Results showed that the amount of AgNPs significantly prevented the formation of electrospun fibers during electrospinning. Thickness, pore size and porosity of the membranes are depicted in Table 1. Thickness of the membranes as measured by a micrometer ranged from 1.40 – 1.70 mm using 10 mL of composite solution. Porosity size and porosity were calculated following equation (1). Pore size of the composite membranes tended to decrease as fiber diameter increased. All samples had good porosity due to well-developed interstices by the interlayered structure among fibers [11]. Membrane porosity increased with the increasing fiber diameter, which plays an important role in determining membrane porosity and pore size.

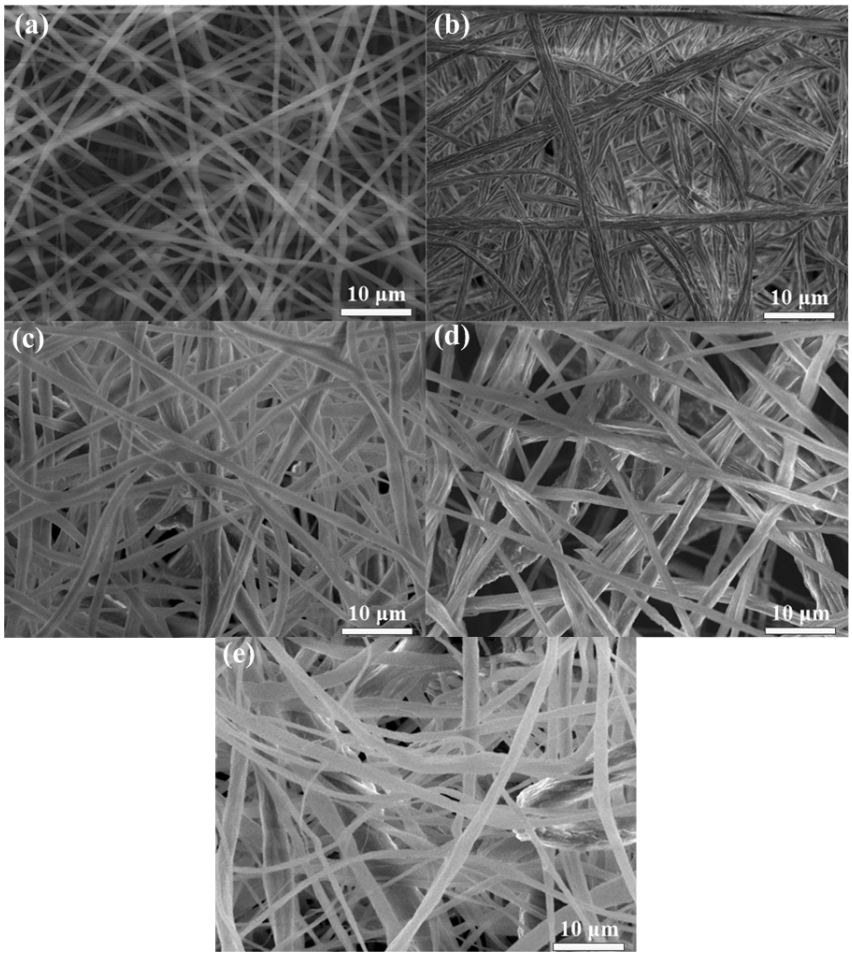

Fig. 2 FESEM image of fibrous membrane: (a) PVDF/PVP, (b) PVDF/PVP/CS/AC membrane containing AgNPs at 0.20, (c) 0.30, (d) 0.40, and (e) 0.50 %v v^{-1}.

Table 1 Thickness, pore size, and porosity of the fibrous membrane

Membrane	Thickness (mm)	Pore size (µm)	Porosity (%)
PVDF/PVP	1.57 ± 0.03	0.24 ± 0.04	79.83 ± 2.32
Ag200	1.68 ± 0.02	0.31 ± 0.06	82.85 ± 3.14
Ag300	1.52 ± 0.03	0.38 ± 0.06	83.87 ± 3.50
Ag400	1.42 ± 0.04	0.42 ± 0.05	85.86 ± 1.41
Ag500	1.54 ± 0.05	0.58 ± 0.07	89.80 ± 3.15

The absorption spectrum of AgNPs was carried out by UV-Vis spectroscopy as shown in Fig. 3(a). Characteristic peak of surface plasmon resonance (SPR) band was found at 389 nm. The absorption peak at 214 nm was ascribed to the formation of various types of silver ions such as Ag^{2+} and Ag^{3+} due to clustering [12]. Broadness of the peaks exhibited that the scattering was caused by a small number of large particles simultaneously formed in solution [13].

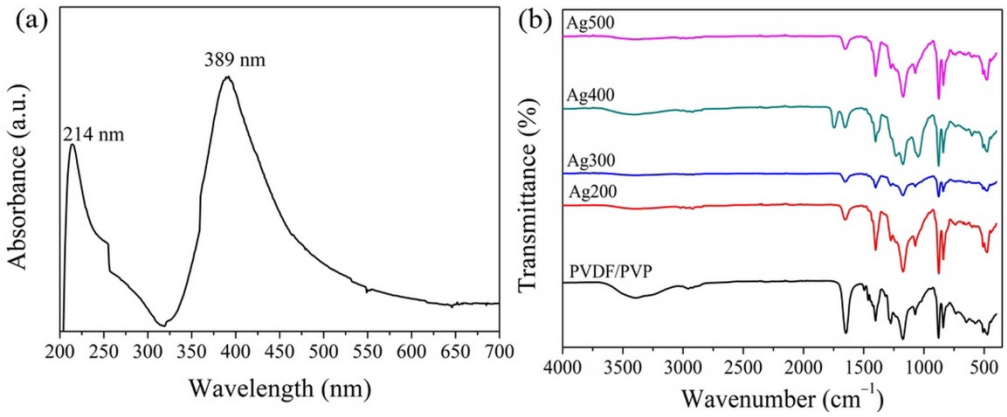

Fig. 3 (a) Absorbance spectrum of AgNPs and (b) ATR-FTIR spectra of composite membranes with different AgNP contents.

Absorption spectra of the membranes were analyzed using ATR-FTIR as shown in Fig. 3(b). Characteristic peaks at 879, 1,175, and 1,402 cm^{-1} were attributed to PVDF [8]. ATR-FTIR spectra at 1402 and 1073 cm^{-1} were attributed to deformation vibration of CH_2 and stretching band of C–C in the β–phase, respectively [14]. The CF_2 bending vibration of PVDF was observed at 473 and 508 cm^{-1} [8]. Broad peaks at 3,393 and 1648 cm^{-1} were ascribed to O–H stretching and C═O stretching vibrations of PVP, respectively [15]. The peak at 1,275 cm^{-1} was ascribed to absorption of the tertiary amine group of PVP [16], while peaks at 736 and 879 cm^{-1} were attributed to α and β–phase groups from PVDF, respectively [17]. Characteristic peaks of chitosan at around 1,600 and 1,000 cm^{-1} corresponding to primary amine N–H bending and C–N stretching disappeared, indicating small amounts of chitosan in the composite membranes [18]. The peak at 1,274 cm^{-1} was assigned to C–O–C stretching vibration [19]. Adding AgNPs in the composite membrane gradually decreased the intensity; the C═O stretching vibration shifted from 1,648 to 1,655 cm^{-1}, indicating chemical interaction between Ag^+ and C═O groups of PVDF/PVP chains [20]. However, the ATR-FTIR spectrum of AC could not be clearly distinguished.

Table 2 Pore size of the fibrous membranes after the filtration method

Membrane	Size of silica particles (μm)
PVDF/PVP	0.212
Ag200	0.240
Ag300	0.201
Ag400	0.332
Ag500	0.306

Composite fibrous membranes were evaluated by silica particles with size ranging from 0.20 – 0.60 μm. Pore size and performance of the filtration test were assessed using a glass vacuum filter with results demonstrated in Table 2. After filtration, silica particles with size range of 0.20 – 0.35 μm were detected, indicating that the composite membranes allowed passage of silica particles lower than 0.30 μm. Results indicated that bacteria with size of 0.45 μm (*E.coli* and *S. aureus*) could not penetrate the composite membrane.

Fig. 4 shows photographs of the antibacterial activity test against *E.coli* and the surviving colonies on the Petri dish. The innumerable colonies on the Petri dish indicated that the PVDF/PVP membrane did not show significant antibacterial activity against *E. coli* (Fig. 4(a)). After the filtration test, there were no surviving colonies on the Petri dish prepared by electrospinning as shown in Fig. 4(b – e). Thus, antibacterial activity against *E. coli* was improved by addition of AgNPs to the composite membrane which showed antibacterial activity against *E. coli* even at low AgNP content of 0.20 v v^{-1}.

Fig. 5 shows antibacterial activity of the composite membrane against *S. aureus*. Results showed that composite membrane containing AgNPs had no antibacterial activity against *S. aureus* due to the number of surviving colonies found alter filtration. Composite membrane had higher antibacterial activity against gram-negative *E. coli* than gram-positive *S. aureus*. Higher antibacterial activity may be due to the effect of sizes of AgNPs. Smaller sized nanoparticles possess larger surface area causing high antibacterial performance [19]. Results showed that gram-negative *E.coli* was more susceptible to silver ions than gram-positive bacteria (*S. aureus*). The main reason for this difference between the results for *E. coli* and *S. aureus* was their gram-positive and gram-negative variance. However, the exact mechanism of action for AgNPs and silver ions (Ag^+) on gram-negative and gram-positive bacteria remains unclear. In general, metallic silver, Ag^+ and AgNPs cause morphological and structural changes in bacterial cells [21]. Antibacterial activities of Ag^+ and AgNPs against bacteria were explained by 2 reasons; first, Ag^+ causes inactivation of cellular proteins by annihilating DNA replication ability [21], and second, electrostatic interaction between negatively charged bacterial membranes and positively charged silver ions can easily enter into and penetrate through the bacterial cells, resulting in protein denaturation in *E.coli* [21]. The antibacterial activity of Ag is not completely understood, although several researchers have indicated the importance of Ag ion release and oxidation of Ag particle surface when in contact with dispersing media [22]. Results showed excellent antibacterial performance of composite membranes fabricated by electro spinning.

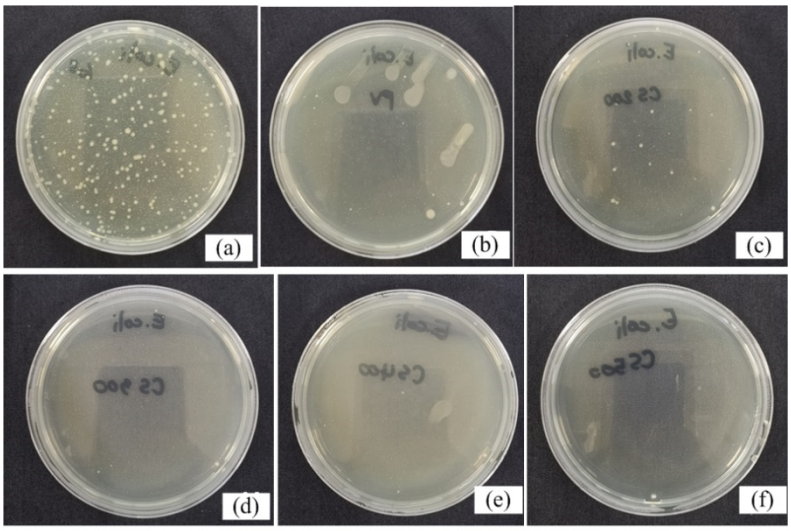

Fig. 4 Photographic images of composite membranes incubated with *E. coli*: (a) PVDF/PVP, (b) PVDF/PVP/CS/AC membrane containing AgNPs at 0.20, (c) 0.30, (d) 0.40, and (e) 0.50 %v v^{-1}.

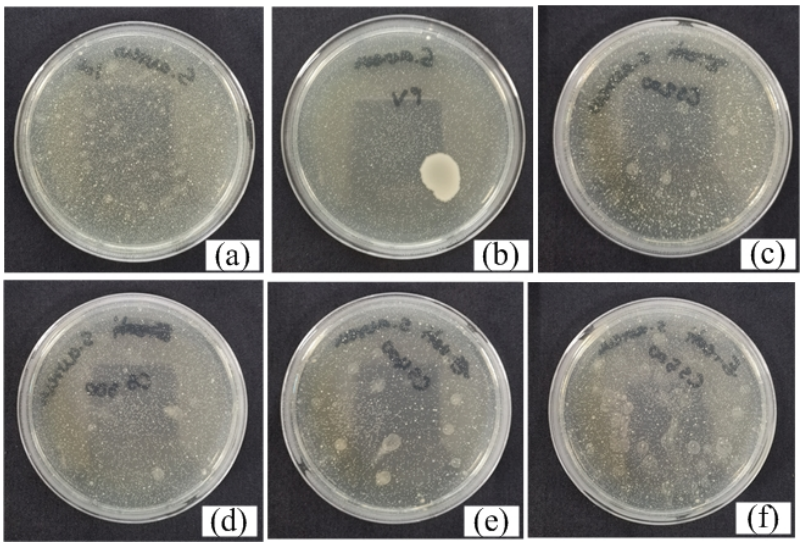

Fig. 5 Photographic images of composite membranes incubated with *S. aureus*: (a) PVDF/PVP, (b) PVDF/PVP/CS/AC membrane containing AgNPs at 0.20, (c) 0.30, (d) 0.40, and (e) 0.50 %v v^{-1}.

4. Conclusion

PVDF/PVP/chitosan/activated carbon/AgNPs nanofiltration membranes were successfully fabricated by electrospinning. Different amount of AgNPs were evaluated for antibacterial activity against *E. coli* and *S. aureus*. Results showed that the porosity of composite membranes increased as fiber diameter increased. Pore sizes of silica particles ranging from 0.20 – 0.35 μm were found after filtration with composite membranes. Composite membranes exhibited excellent antibacterial activity against *E.coli* even at low AgNP contents. Results indicated that addition of AgNPs in composite membranes improved bacterial activity as feasible candidates for drinking water and wastewater treatment.

5. Acknowledgements

This work was financially supported by Ubon Ratchathani Rajabhat University and National Research Council of Thailand (Grant No. 11965).

6. References

[1] Y. Ji, W. Qian, Y. Yu, Q. An, L. Liu, Y. Zhou, C. Gao, Recent developments in nanofiltration membranes based on nanomaterials, Chin. J. Chem. Eng. 25(2017) 1639 – 16521.
[2] F.E. Ahmed, B.S. Lalia, R. Hashaikeh, A review on electrospinning for membrane fabrication: Chalenges and application, Desalination. 356 (2015) 15 – 30.
[3] G.D. Kang, Y.M. Cao, Application and modification of poy (vinyllidene fluoride)(PVDF) membrane-A review, J. Membr. Sci. 463 (2014) 145 – 165.
[4] A.W. Jatoi, I.S. Kim, H. Ogasawara, Q.Q. Ni, Characterizations and application of CA/ZnO/AgNP composite nanofibers for sustained antibacterial properties, Mater. Sci. Eng. C. 105 (2019) 110077.
[5] R. Alipour, A. Khorshidi, A.F. Shojaei, F. Mashayekhi, M.J.M. Moghaddam, Skin wound healing acceleration by Ag nanoparticles embedded in PVA/PVP/Pectin/Mafenide acetate composite nanofibers, Polym. Test. 79 (2019) 106022.
[6] K. Li, S. Cui, J. Hu, Y. Zhou, Y. Liu, Crosslinked pectin nanofibers with well-dispersed Ag nanoparticles: Preparation and characterization, Carbohydr. Polym. 199 (2018) 68 – 74.

[7] A. Ali, M.A. Shahid, M.D. Hossain, M.N. Islam, Antibacterial bi-layered polyvinyl alcohol (PVA)-chitosan blend nanofibrous mat loaded with *Azadirachta indica* (neem) extract, Int. J. Biol. Macromol. 138 (2019) 13 – 20.

[8] S.M. Lamine, C. Ridha, H. M. Mahfoud, C. Mouad, B. Lotfi, A.H. Al-Dujaili, Chemical activation of an activated carbon prepared from coffee residue, Energy Procedia 50 (2014) 393 – 400.

[9] K. Li, D. Hou, C. Fu, K. Wang, J. Wang, Fabrication of PVDF nanofibrous hydrophobic composite membranes reinforced with fabric substrates via electrospinning for membrane distillation desalination, J. Environ. Sci. 75 (2019) 277 – 288.

[10] D.H. Kang, H.W. Kang, Surface energy characteristics of zeolite embedded PVDF nanofibers films with electrospinning process, Appl. Surf. Sci. 387 (2016) 82 – 88.

[11] Y.J. Kim, C.H. Ahn, M.O. Choi, Effect of thermal treatment on the characteristics of electrospun PVDF−silica composite nanofibrous membrane, Eur. Polym. J. 46 (2010) 1957 – 1965.

[12] P.K. Khanna, N. Singh, D. Kulkarni, S. Deshmukh, S. Charan, P.V. Adhyapak, Water based simple synthesis of re-dispersible silver nano-particles, Mater. Lett. 61 (2007) 3366 – 3370.

[13] G.L. Flower, S.V. Latha, K.V. Rao, Novel characterization of nanosilver fluid through ultrasonic studies supported by UV–Vis spectroscopy, DLS and TEM studies, J. Mol. Liq. 221 (2016) 333 – 338.

[14] N. Wu, Q. Cao, X. Wang, Q. Chen, Study of a novel porous gel polymer electrolyte based on TPU/PVdF by electrospinning technique, Solid State Ion. 203 (2011) 42 – 46.

[15] C. Peng, G. Li, D.l. Geng, M. Shang, Z. Hou, J. Lin, Fabrication and luminescence properties of one-dimensional $ZnAl_2O_4$ and $ZnAl_2O_4$: A^{3+} (A = Cr, Eu, Tb) microfibers by electrospinning method, Mater. Res. 47 (2012) 3592 – 3599.

[16] C. Peng, G. Li, D.l. Geng, M. Shang, Z. Hou, J. Lin, Fabrication and luminescence properties of one-dimensional $ZnAl_2O_4$ and $ZnAl_2O_4$: A^{3+} (A = Cr, Eu, Tb) microfibers by electrospinning method, Mater. Res. Bull. 47 (2012) 3592 – 3599.

[17] A.M. Zahari, C.W. Shuo, P. Sathishkumar, A.R.M. Yusoff, F.L. Gu, N.A. Buang, L. Woei-Jyec, R.J. Gohari, Z. Yusop, A reusable electrospun PVDF-PVP-MnO_2 nanocomposite membrane for bisphenol A removal from drinking water, J. Environ. Chem. Eng. 6 (2018) 5801 – 5811.

[18] M.B. Stie, M. Jones, H.O. Sørensen, J. Jacobsen, I.S. Chronakis, H.M. Nielsen, Acids 'generally recognized as safe' affect morphology and biocompatibility of electrospun chitosan/polyethylene oxide nanofibers, Carbohydr. Polym. 215 (2019) 253 – 262.

[19] J.A. Wahab, I.S. Kim, Q.Q. Ni, A comparative study on synthesis of AgNPs on cellulose nanofibers by thermal treatment and DMF for antibacterial activities, Mater. Sci. Eng. C. 98 (2019) 1179 – 1195.

[20] R. Li, Z. Cheng, X. Yu, S. Wang, Z. Han, L. Kang, Preparation of antibacterial PCL/PVP-AgNP Janus nanofibers by uniaxial electrospinning, Mater. Lett. 254 (2019) 206 – 209.

[21] S. Calamak, E.A. Aksoy, N. Ertas, C. Erdogdu, M. Sagıroglu, K. Ulubayram, Ag/silk fibroin nanofibers: Effect of fibroin morphology on Ag^+ release and antibacterial activity, Eur. Polym. J. 67 (2015) 99 – 112.

[22] K. Matsuyama, K. Morotomi, S. Inoue, M. Nakashima, H. Nakashima, T. Okuyama, et al., Antibacterial and antifungal properties of Ag nanoparticle-loaded cellulose nanofiber aerogels prepared by supercritical CO_2 drying, J. Supercrit. Fluid. 143 (2019) 1 – 7.